CFD Letters

Journal homepage: www.akademiabaru.com/cfdl.html
ISSN: 2180-1363

Mathematical Modelling for Effects of Fineness Ratio, Altitude and Velocity on Aerodynamic Characteristics of an Airship Design using Computational Fluid Dynamics

Open Access

Jafirdaus Jalasabri[1], Fairuz Izzuddin Romli[1,*], Mohammad Yazdi Harmin[1]

[1] Department of Aerospace Engineering, Faculty of Engineering, Universiti Putra Malaysia, Malaysia

ARTICLE INFO

Article history:
Received 23 August 2020
Received in revised form 22 October 2020
Accepted 25 October 2020
Available online 31 October 2020

ABSTRACT

The external shape design change of an airship can be appropriately captured by design fineness ratio, which is defined as the ratio of airship's length to its maximum width. However, there is a lack of aerodynamic models that have been established for airship design purposes. In conjunction to this realization, the aim of this research work is to establish the effects of the design fineness ratio of an airship towards its aerodynamic performance. The Atlant-100 airship is chosen as the reference design model for this study. In total, 36 simulation runs are executed with different combinations of values for design fineness ratio, altitude and velocity. The obtained CFD simulation results are then statistically analysed using Minitab software to evaluate the significance of the design fineness ratio effects. From the results, it was found that smaller fineness ratio corresponds to higher aerodynamic lift and drag forces. As in the case simulated in this study, the smallest fineness ratio of 0.93 was shown to correspond to the highest value of lift coefficient while having comparable drag coefficient with other fineness ratios. This highlights that a smaller fineness ratio of the airship design is more suitable. The constructed mathematical models to capture these effects have also been validated with a few goodness-of-fit tests. For the regression model of fineness ratio impact on the lift coefficient, it has R^2 value of 99.3%. When its predictive accuracy is tested with few simulated random cases, the maximum error obtained is only about 5%. On the other hand, for the regression model of the fineness ratio impact on drag coefficient, the R^2 value is 99.8% and maximum predictive error from the simulation random cases test is only around 11%. Overall, it can be concluded that the constructed regression models have good predictive ability for impact of design fineness ratio on aerodynamic performance of the airship under this study.

Keywords:
Fineness ratio; airship design; aerodynamic performance; mathematical modelling

1. Introduction

When the revolutionary urban "flying bus" idea is proposed recently, airships seem to be the most suitable means for the transportation concept. Airships are no stranger to public transportation field,

[*] *Corresponding author.*
E-mail address: fairuz_ir@upm.edu.my (Fairuz Izzuddin Romli)

https://doi.org/10.37934/cfdl.12.10.90110

having served as the commercial air transportation means since early 1930s. However, with the new technology advancements that have led to much safer airship operation, its recent comeback talks into mainstream passenger air transportation are essentially fuelled by progressive market interests and demands [1]. With these developments and interests on the use of airships as alternative public air transport means, it is possible that they could be operated to alleviate the traffic congestion within urban cities. Figure 1 shows example vision of having airships operating as mass public transportation means in urban cities.

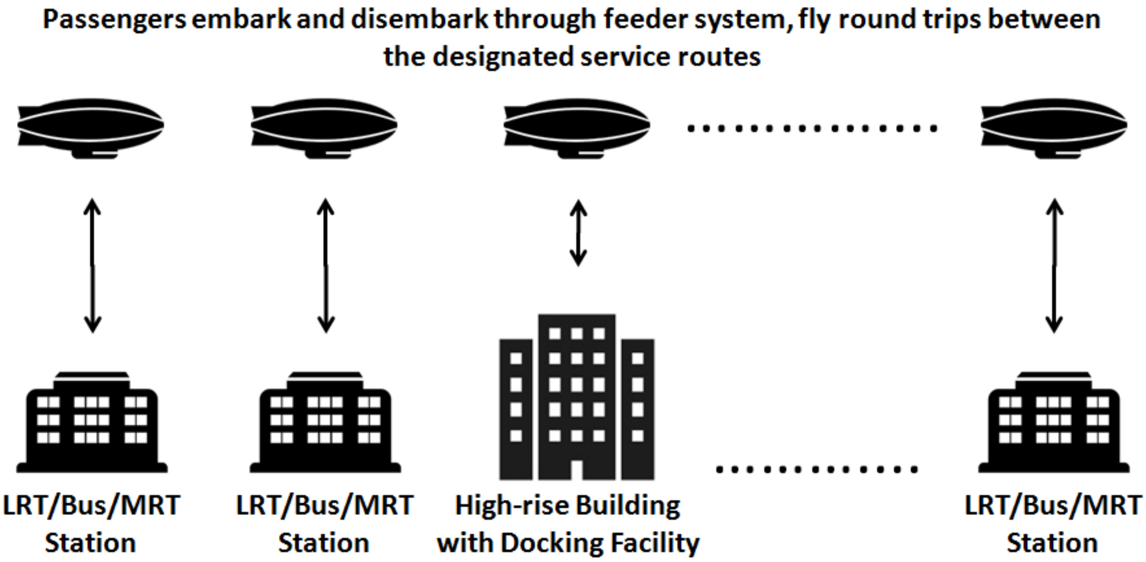

Fig. 1. Visionary mission profile of public transport airships [2]

In engineering design process of an airship, its external shape plays a vital role for its aerodynamic performance. To arrive at the optimal airship design with respect to its mission profile, many external shapes of the airship might need to be considered and tested. Modification of the external shape of an airship can be captured by using the design fineness ratio parameter, which is defined as the ratio of the length of the body against its maximum width. In aerospace design, the fineness ratio was used to describe the overall shape of a streamlined body and it is one of the common design parameters included in aerodynamics, weights and sizing analyses [3]. The impact of fineness ratio parameter on aerodynamic characteristics of a body was demonstrated in several studies including Sahai *et al.,* [4], Kruger *et al.,* [5] and Nicolosi *et al.,* [6]. These studies have shown that different fineness ratios will correspond to different aerodynamic characteristics of the body.

Because of its large size, designing an airship is comparatively expensive and its structure can be hardly modified after complete construction [7]. Hence, the common trial and error design method is highly unsuitable for development of an airship. Instead, for such design cases, the application of mathematical models that capture the effects of changing design parameters is of a great assistance to the designers during the early conceptual design stages. Unfortunately, there is also a general lack of studies that have been done on the aerodynamics of an airship, especially for the current modern hybrid airship designs. Few recent computational and experimental studies that have been done on aerodynamics of an airship include those by Andan *et al.,* [8], Wang *et al.,* [9] and Sun *et al.,* [10]. Hence, it is recognized that there is an ongoing need to construct predictive mathematical models that can be applied in airship design process, especially to aid designers in making the correct design decisions during the early conceptual stage. Since the external shape of the airship plays a significant role in its aerodynamic performance, it is highly beneficial to have the relationship model between its design fineness ratio and aerodynamic performance. With this realization, development of such predictive mathematical models through computational analysis becomes the main objective for the research study presented in this paper.

2. Methodology

For this study, the Atlant-100 modern passenger transport airship was chosen as the reference baseline design. It should be noted that the development of computer-aided design (CAD) model for the Atlant-100 airship is done using available design details within the public domain. Therefore, this CAD model as illustrated in Figure 2 is an approximate model of the Atlant-100 airship. Subsequently, this also means that the obtained results in later computational simulation analyses might not be the actual Atlant-100 airship's performance. However, it is believed that the impact trends from changing the design fineness ratio of the airship to its aerodynamic performance will be closely similar.

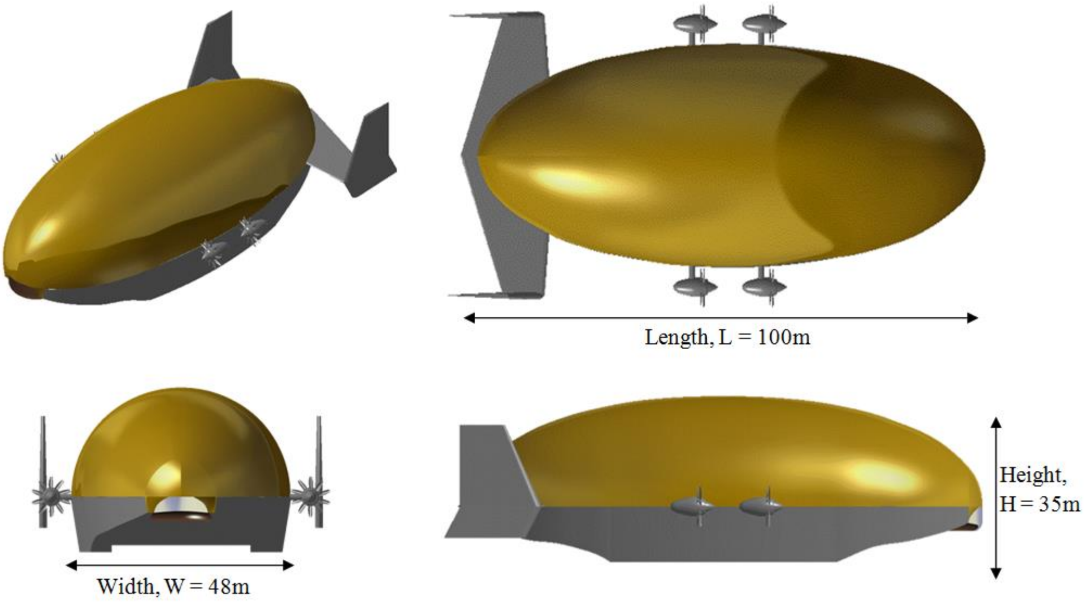

Fig. 2. Approximate CAD model of the reference Atlant-100 airship [11]

Overall methodology for this research study is summarized in Figure 3. In short, the approximate CAD model of the Atlant-100 airship is constructed using CATIA software.

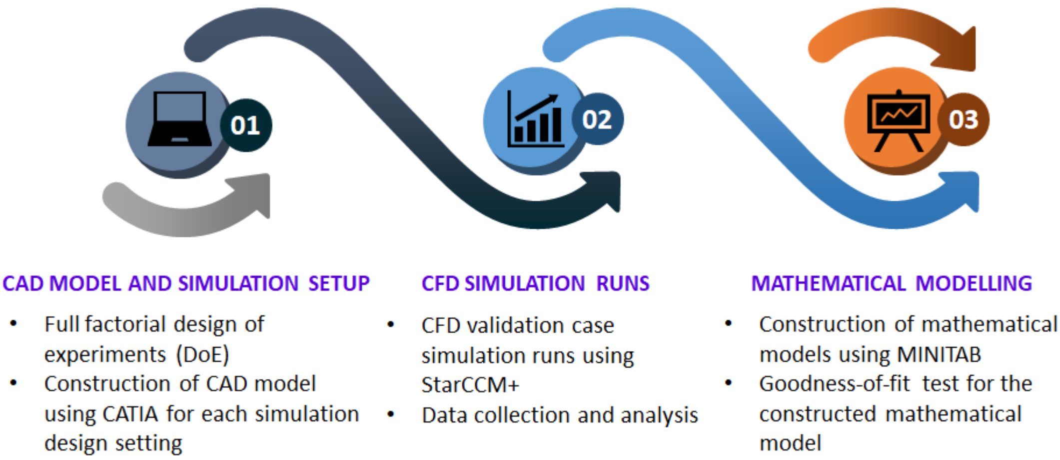

Fig. 3. Main steps of the research methodology for this study

The model is then used in computational fluid dynamics (CFD) simulation analysis that is conducted StarCCM+ software. CFD is essentially a branch of fluid mechanics that applies numerical analysis and data structures in order to study and solve problems involving fluid flows, which has found a significant importance in design engineering process. Among others, the CFD method was applied in many studies including for the vertical pipe [12], wind turbine blades [13] and aircraft's inboard store [14]. A total of 36 simulation runs are executed with different combinations of fineness ratio, altitude and velocity. The settings of the case runs are dictated from design of experiment (DoE) method at full factorial combination. The obtained CFD simulation results are then statistically analysed using the Minitab software to evaluate the significance of effects on aerodynamic performance of the airship by fineness ratio, altitude and velocity, and to formulate the mathematical models that capture these effects.

2.1 Turbulence Model Selection

There are several available turbulence models that can be applied in CFD analysis. For this study, the turbulence model is chosen by comparing their performance in an example simulation case study of the NACA 0012 aerofoil. CFD simulation results for lift and drag coefficients from using different turbulence models are compared with the values from experimental analysis in published research work by Jespersen *et al.,* [15] and Ahmed *et al.,* [16]. The CFD simulation settings have been tailored to the experimental settings in these two references: angle of attack of three degrees, Mach number of 0.15 (velocity of about 43.82 m/s) and also Reynold's number of 6 million in a compressible flow environment. Figure 4 depicts the results of the mesh study done for this comparison case study, which shows variation of lift coefficient for the NACA 0012 aerofoil against number of cells. As can be observed from the plot, the solution seems to converge when number of cells is more 7.5 million. Hence, it is taken that the meshing in this particular case study should roughly have at least 7.5 million cells in order to have accurate CFD results.

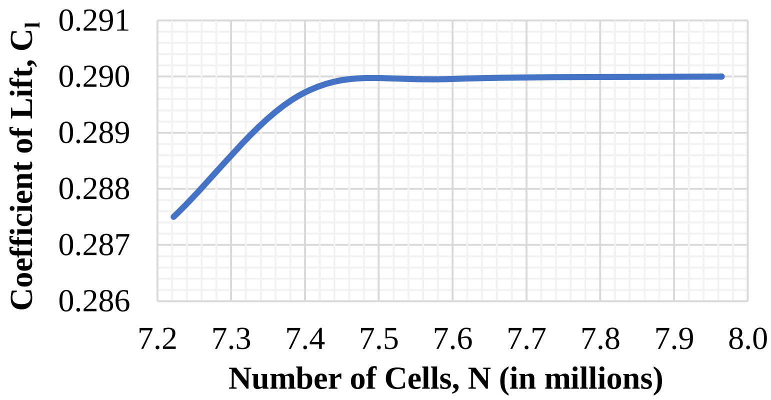

Fig. 4. Lift coefficient against number of cells

The CFD simulation results for lift coefficient of the NACA 0012 are depicted in Figure 5 and they are also tabulated in Table 1. It should be noted the obtained simulation results are consistent with the published results in a similar study by Eleni *et al.,* [17]. From Table 1, it can be seen that the value of lift coefficient obtained using the standard Spalart-Allmaras turbulence model has the lowest error percentage in comparison to the value from actual experiment, which is taken as 0.3. This indicates that this turbulence model has performed the best in the simulation of lift coefficient for the NACA 0012 aerofoil.

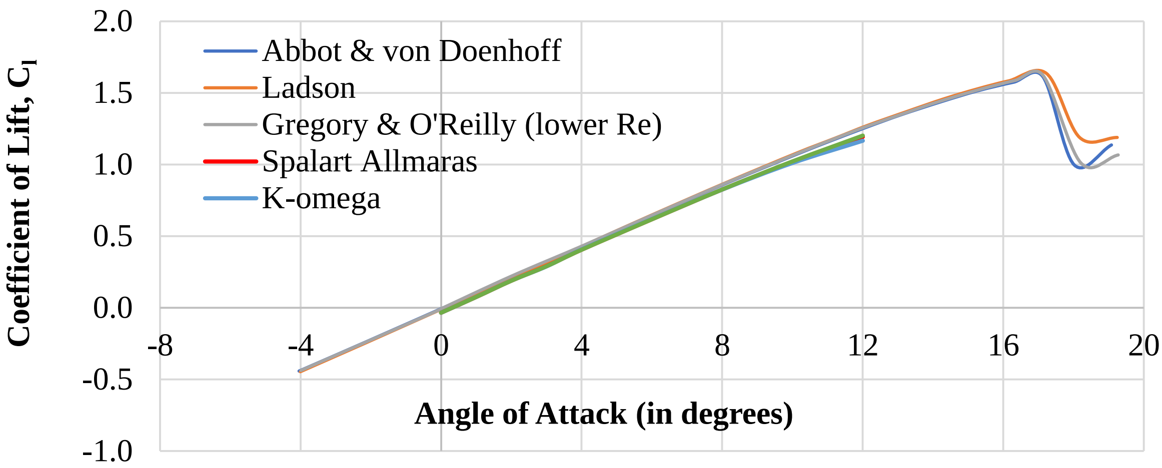

Fig. 5. Comparison of experimental and simulation results for lift coefficient of NACA 0012 aerofoil

Table 1
Experimental and simulation results for lift coefficient of NACA 0012 aerofoil

Turbulence Model	Simulated Lift Coefficient	% Error to Experimental Result
K-Epsilon	0.2897	3.43
K-Omega	0.2895	3.50
Standard Spalart-Allmaras	0.2905	3.17

Furthermore, performance of standard Spalart-Allmaras in producing good drag coefficient value against that from the actual experimental value is also studied. The experimental result for the drag coefficient of NACA 0012 aerofoil at lift coefficient equals to 0.3 for similar simulation setting is about 0.0095. Meanwhile, based on the simulation analysis using standard Spalart-Allmaras, the simulated value of drag coefficient is 0.0106. This over-prediction of drag coefficient is anticipated and can be contributed to the capability of the standard Spalart-Allmaras turbulence model in capturing airflow behaviour around the body and also the calculation method that it applies to solve the Navier-Stokes equation, particularly for near wall analysis. In Figure 6, a similar pattern of the airflow on top of the NACA 0012 aerofoil can be observed for all turbulence models when velocity is over 50 m/s.

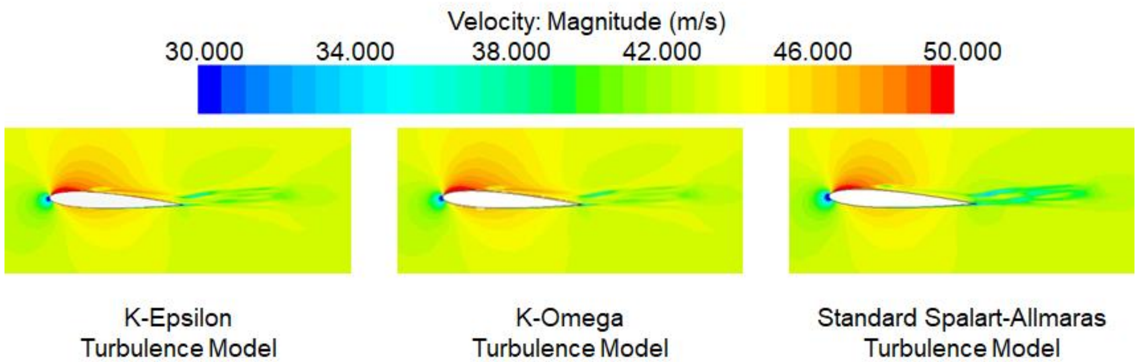

Fig. 6. Velocity plot for NACA 0012 aerofoil simulation using different turbulence models at 3-degree angle of attack

However, the standard Spalart-Allmaras turbulence model seems to have a better ability to capture turbulent airflow at the trailing edge compared to other turbulence models. Unfortunately, this also typically leads to over-prediction of the turbulent flow and produces the far less efficient prediction of airflow around the wing. As a result, the use of the standard Spalart-Allmaras model is unable to accurately capture the detailed force, resulting in a notable error percentage for the drag coefficient value. On the other hand, the standard Spalart-Allmaras model is more superior in capturing the shear forces in comparison to other models, which enables a better prediction of the lift force behaviour. Based on these arguments, it is taken that the standard Spalart-Allmaras is a suitable turbulence model to be applied in this study.

2.2 Meshing Study

For the initial meshing study, the classic Zeppelin model used was constructed with matching dimensions to the ones applied in previous study by Voloshin *et al.,* [18]. The CAD model is shown in Figure 7, which has a fineness ratio of 4:1 with approximate chord length of 1 m and location of centre of gravity is on the axis of symmetry at a distance of 0.451 m from the nose, plus the angle of attack is set to be -0.4 degrees. Further details regarding the simulation environment settings are tabulated in Table 2, which are all tailored to previous study by Voloshin *et al.,* [18]. By doing this, the obtained simulation results can be compared to the ones published in this previous study.

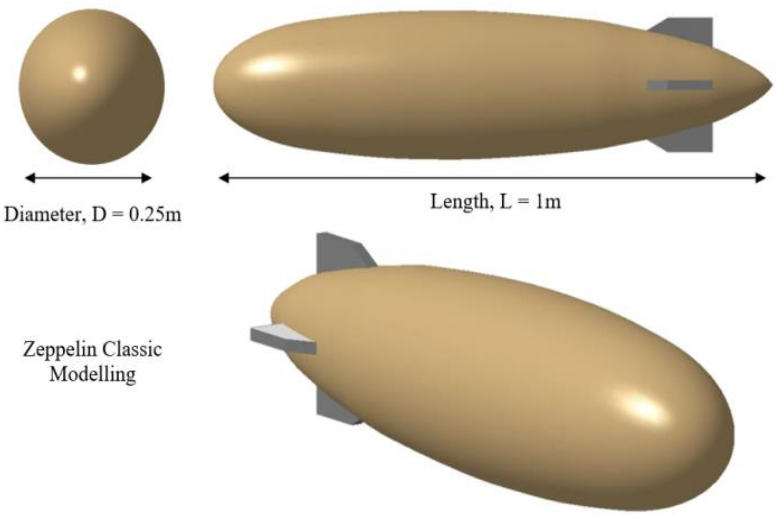

Fig. 7. Classic Zeppelin modelling in CATIA

Table 2
Environment settings for meshing study

Parameter	Setting Value
Dimension	1 m × 0.25 m
Reference Area, S	0.101 m^2
Reference Length, l	1 m
Fineness Ratio	4:1
Constant Density, ρ	1.204 kgm^{-3}
Dynamic Viscosity, µ	1.789×10^{-5} Pa.s
Ambient Pressure at Sea Level	101325 Pa
Airship Velocity, v	37 ms^{-1}
Angle of Attack	-0.4^o
Turbulence Model	Standard Spallart-Allmaras
Simulation Types	Steady-state
No. Simulation Iterations	1500

The considered trimmer and polyhedral mesh types are illustrated in Figure 8. Both have constant number of layers, 10 layers near-wall prism with 8 mm mesh size and the maximum size of meshing cells is 64 mm on the analysis environment. By observing Figure 8, it appears that the trimmer mesh (structured mesh) produces more organized shape as the layers become much smaller when they are closer to the model, unlike for the polyhedral mesh. This situation is mainly due to significant effects of the boundary layers, which lead to more detailed mesh levels. It was stated that this mesh is able to produce balanced calculation in each node as the size is constantly the same [18]. In contrast, the polyhedral mesh fills the environment block with different shapes and sizes. They might yield better result since they consist more nodes in each cell with different boundary layers. For this reason, they can produce more accurate cells calculation but with an unbalanced number of nodes configuration.

As observed in Table 3, the value of simulated drag coefficient for both types of mesh seems to be far less accurate than for lift coefficient. It is noted that the pressure forces contribute the biggest effect (about 98%) to lift coefficient while the shear forces are the big contributor to drag coefficient (about 90%) [18]. Since the prediction of shear forces is more difficult to do in comparison to pressure forces, a larger error for drag coefficient was expected. Both mesh types need to have more boundary layers and smaller mesh size in order to better capture the airflow.

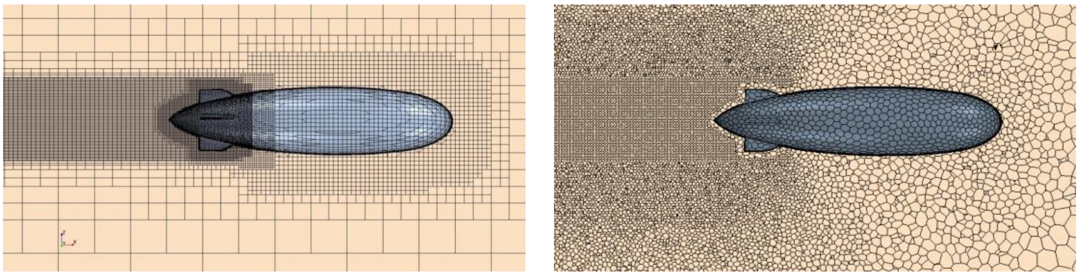

(a) (b)

Fig. 8. (a) Trimmer mesh (b) Polyhedral mesh

Table 3
Results for meshing simulation study

Type of Mesh	No. of Cells (x 10^6)	C_l	C_d
Experimental	-	0	0.0419
Polyhedral [15]	4.5	-0.0080	0.0390
Trimmer	4.0	-0.0021	0.0225
Polyhedral	4.7	-0.0020	0.0270

The error from using structured trimmer mesh is higher than that for unstructured polyhedral mesh and this can be explained by looking at Figure 9. The polyhedral mesh results in a more accurate result because it is the best option to steep filleted or rounded surface such as the shape of Zeppelin or airship. It can be observed that the resultant contour plots are only slightly different to each other, especially in region of the body surface and tail (near boundary layers). Nonetheless, the differences result in different behaviour of the turbulence airflow whereby the separation airflow at the rear airship body in the case of the polyhedral mesh is much more detailed in comparison to that of the trimmer mesh. With polyhedral mesh, the airflow is separated block-by-block at the wake area since there are more cells in the block area. In contrast, the trimmer mesh produces a smooth-filled line. Moreover, in terms of the wall shear stress, the polyhedral mesh produces reddish-coloured pressure contour at the fin area as a result of more detailed airflow calculation on each of its nodes. Overall, it appears that the number of nodes provides particularly different airflow behaviour for each type of mesh and the polyhedral mesh gives more details in capturing pressure and velocity. Hence, the polyhedral mesh is chosen to be applied for this research study.

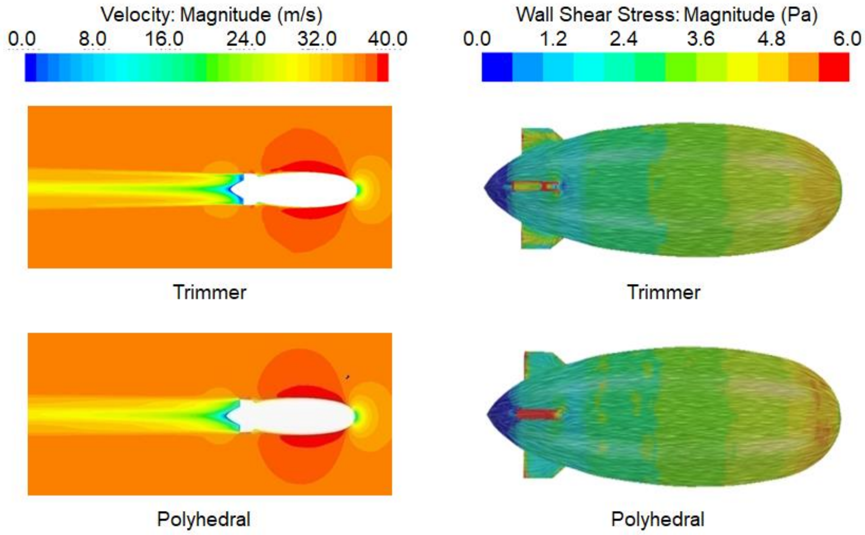

Fig. 9. Velocity plot and wall shear stress vector diagram

2.3 Simulation Settings

In the simulation analysis, the airship design model is varied in terms of its design fineness ratio. Moreover, the settings of both altitude and velocity are also changed to observe their impact on the aerodynamic performance of the airship. The range of altitude and velocity is chosen based on the expected value for operation of mass transportation airship. Design of experiments (DoE) method is applied to set the settings for each simulation run in this study to ensure that the simulation data can be properly used for the mathematical modelling process in the following step of the methodology. Overall, in full factorial DoE setup, the total number of simulation runs for this study is 36, with three levels for design fineness ratio and altitude parameters while velocity parameter has four levels. By referencing the previous study by Battipede *et al.,* [19], the simulation environment was set up as presented in Table 4 and Figure 10, where L is length of the airship.

Table 4
Simulation environment physical and mesh setup

Parameter	Setting Value
Constant Density, ρ	1.204 kgm^{-3}
Dynamic Viscosity, μ	1.789 x 10^{-5} Pa.s
Ambient Pressure at Sea Level	101325 Pa
Airship Velocity, v	37 ms^{-1}
Angle of Attack	-0.4°
Turbulence Model	Standard Spallart-Allmaras
Cells Size	> 7.5 millions
Simulation Types	Steady-state
No. Simulation Iterations	1500

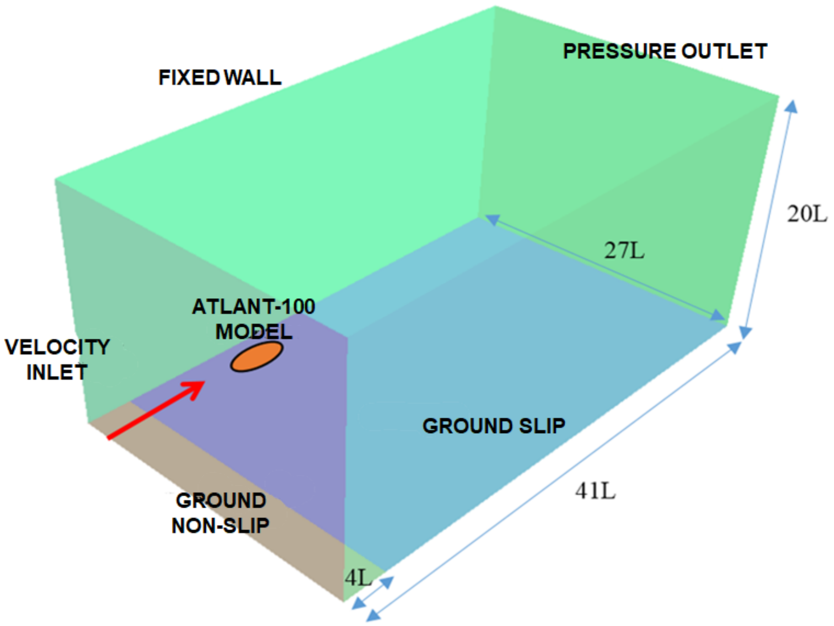

Fig. 10. Simulation environment domain setup (with L = 100 m)

The design fineness ratio here is defined as the ratio of the design length divided by its diameter. Three variations of design fineness ratio value are being considered in this study, which means the reference Atlant-100 airship design is modified in correspondence to the three considered design fineness ratio settings. The dimensions and the frontal area values downward in Z-direction for the different scaled Atlant-100 airship models to the different fineness ratios are indicated in Figure 11. It should be noted that only the width of the reference Atlant-100 airship design is modified to change its design fineness ratio while the other dimensions are kept constant. It is observed that the Atlant-100 airship design becomes bulkier as its width is increased (or with smaller fineness ratio).

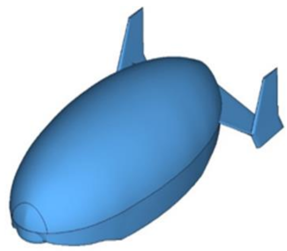

Design Fineness Ratio = 2.08
Dimensions (L x W x H) = 100 m x 48 m x 35 m
Frontal Area = 4481.6 m^2

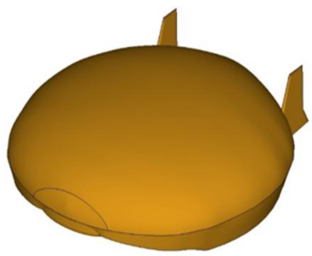

Design Fineness Ratio = 1.39
Dimensions (L x W x H) = 100 m x 78 m x 35 m
Frontal Area = 6301.4 m^2

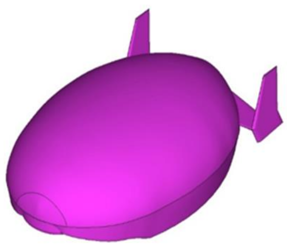

Design Fineness Ratio = 0.93
Dimensions (L x W x H) = 100 m x 108 m x 35 m
Frontal Area = 9073.5 m^2

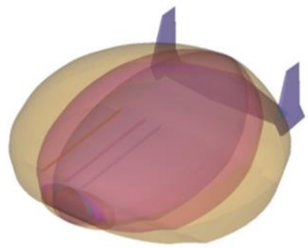

Expansion of width by scaling up ratio of 1.5 for the three cases

Fig. 11. Constructed CAD models for different design fineness ratios

2.4 Mathematical Modelling

The collected data from the CFD simulations is used to fit the mathematical regression model for the relationship of fineness ratio, altitude and velocity with the resultant aerodynamic lift and drag coefficients of the airship. In this study, the regression analysis is done using the MINITAB statistical software, where the regression fit is done separately for lift and drag coefficients as the dependent variables while fineness ratio, altitude and velocity as the independent variables. Once the regression models have been constructed, they will be subjected to several goodness-of-fit tests to ensure that the models fit the data well. Among the tests that were applied to measure goodness of the model include R^2 value, Analysis of Variance (ANOVA), residual plots and using several random test cases to observe the error between the actual values and the fitted values by the regression model.

3. Results and Discussion

The obtained CFD simulation results are tabulated in Table 5. In general, it can be observed that the airship design model with lower design fineness ratio produces higher lift and drag coefficients. This was expected as a wider airship body with same length can generate more lift force due to more exposed surface area.

3.1 Effect of Altitude on Lift and Drag Coefficients

When altitude is increased, the atmospheric density and Reynold's number will decrease [20]. As a result, the generated lift coefficient will also decrease as density, dynamic viscosity, pressure and temperature of atmospheric air environment are all decreased with altitude. This can be seen in the plots of simulated lift coefficient for different altitudes as shown in Figure 12 at different velocities. From the plots, there is no consistent trend that can be visibly captured with increasing altitudes for all different velocities studied. The explanation for this situation can be contributed to the variation of the hull body and wing tail design of the modified airship models. However, larger fineness ratio model (i.e. smaller body width) consistently corresponds to lower lift coefficient for all velocities. The modified airship model with higher design fineness ratio lacks lifting surface (else known as projected area), which is meant to capture the aerodynamic lift produced by the hull body. Airship model with a high fineness ratio mostly has to generate additional lift from the wing due to its smaller hull body. In a nutshell, the larger the fineness ratio of the airship, the slender its hull body becomes and hence less lift force can be generated. Another observation from the simulation results highlights that the lift force generation is much more consistent at higher altitudes than lower ones due to decrement of environmental pressure and shear force as the altitude is increased.

Meanwhile, plots of the simulated drag coefficient for different altitudes are presented in Figure 13 at different velocities. Unlike lift coefficient, the trend for drag coefficient is essentially consistent. It can be seen that the modified Atlant-100 airship model with design fineness ratio of 1.39 produces the highest aerodynamic drag coefficient compared to other ratios. This is mainly due to the presence of more downward airflows (as observed during simulation run), which occurs because the model's wing size is smaller at this fineness ratio. When the fineness ratio is 2.08 and 0.93, negative direction of the force coefficient from wing section occurs. This means that contribution of wing is less towards the wake formation at the back of the airship as can be seen from Figure 14. In contrast, for airship's design fineness ratio of 1.39, the generated force coefficient from wing section was mostly positive at different combinations of altitude and velocity, which adds to the total drag force of the airship.

As a result of the combination of the aerodynamic airflow on the hull body that directs higher airflow, negative direction of force is created and hence a higher drag force around the wing area.

Table 5
Simulation analysis results from StarCCM+

Run	Fineness Ratio	Altitude (m)	Velocity (km/h)	C_L	C_D
1	2.08	1500	100	0.026	0.024
2	2.08	1500	140	0.039	0.026
3	2.08	1500	190	0.039	0.027
4	2.08	1500	250	0.032	0.025
5	2.08	2000	100	0.029	0.026
6	2.08	2000	140	0.025	0.023
7	2.08	2000	190	0.031	0.026
8	2.08	2000	250	0.040	0.026
9	2.08	2500	100	0.040	0.027
10	2.08	2500	140	0.022	0.025
11	2.08	2500	190	0.017	0.023
12	2.08	2500	250	0.042	0.025
13	1.39	1500	100	0.048	0.036
14	1.39	1500	140	0.044	0.032
15	1.39	1500	190	0.047	0.033
16	1.39	1500	250	0.040	0.031
17	1.39	2000	100	0.038	0.036
18	1.39	2000	140	0.047	0.034
19	1.39	2000	190	0.055	0.034
20	1.39	2000	250	0.047	0.037
21	1.39	2500	100	0.052	0.036
22	1.39	2500	140	0.055	0.036
23	1.39	2500	190	0.054	0.036
24	1.39	2500	250	0.047	0.035
25	0.93	1500	100	0.055	0.033
26	0.93	1500	140	0.089	0.037
27	0.93	1500	190	0.069	0.033
28	0.93	1500	250	0.088	0.036
29	0.93	2000	100	0.061	0.033
30	0.93	2000	140	0.070	0.035
31	0.93	2000	190	0.060	0.032
32	0.93	2000	250	0.078	0.036
33	0.93	2500	100	0.059	0.032
34	0.93	2500	140	0.058	0.032
35	0.93	2500	190	0.072	0.035
36	0.93	2500	250	0.078	0.036

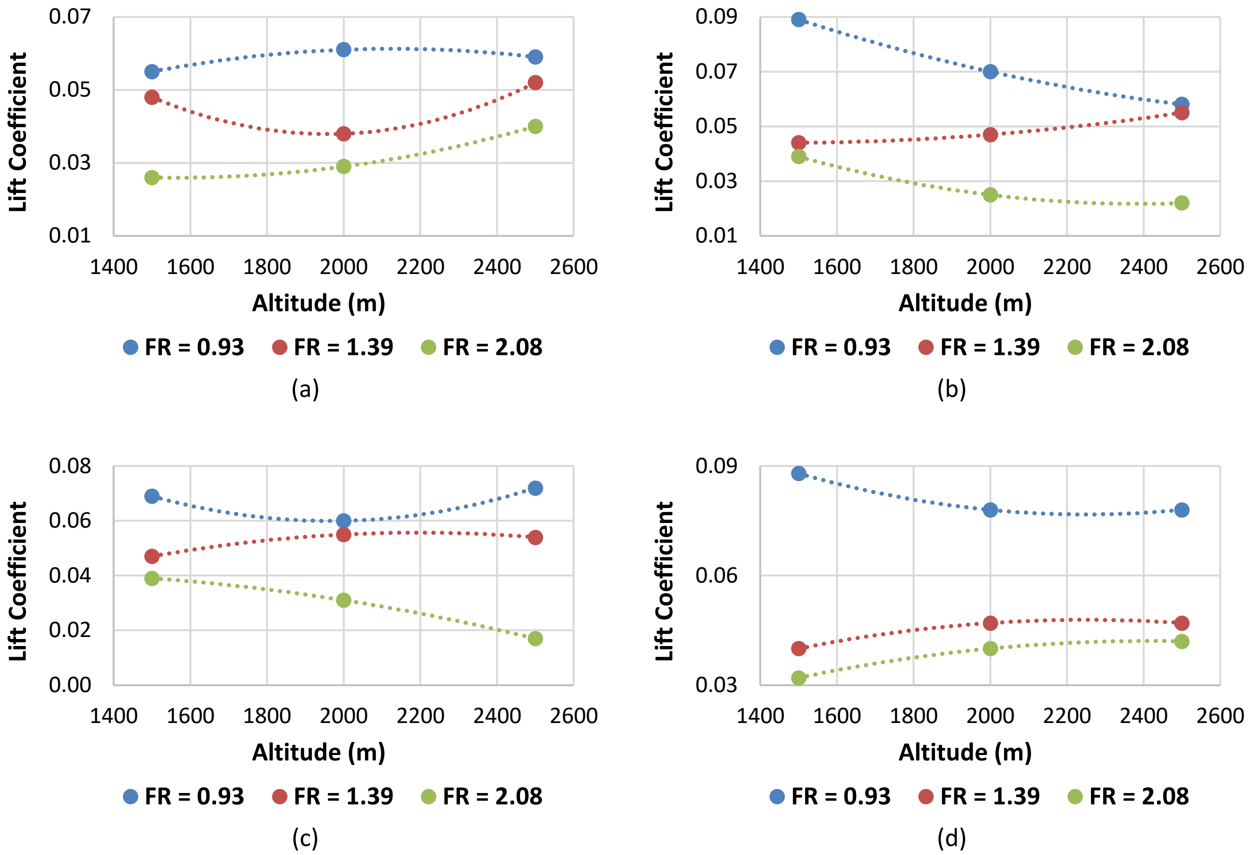

Fig. 12. Lift coefficient for different altitudes at (a) 100 km/h; (b) 140 km/h; (c) 190 km/h; (d) 250 km/h

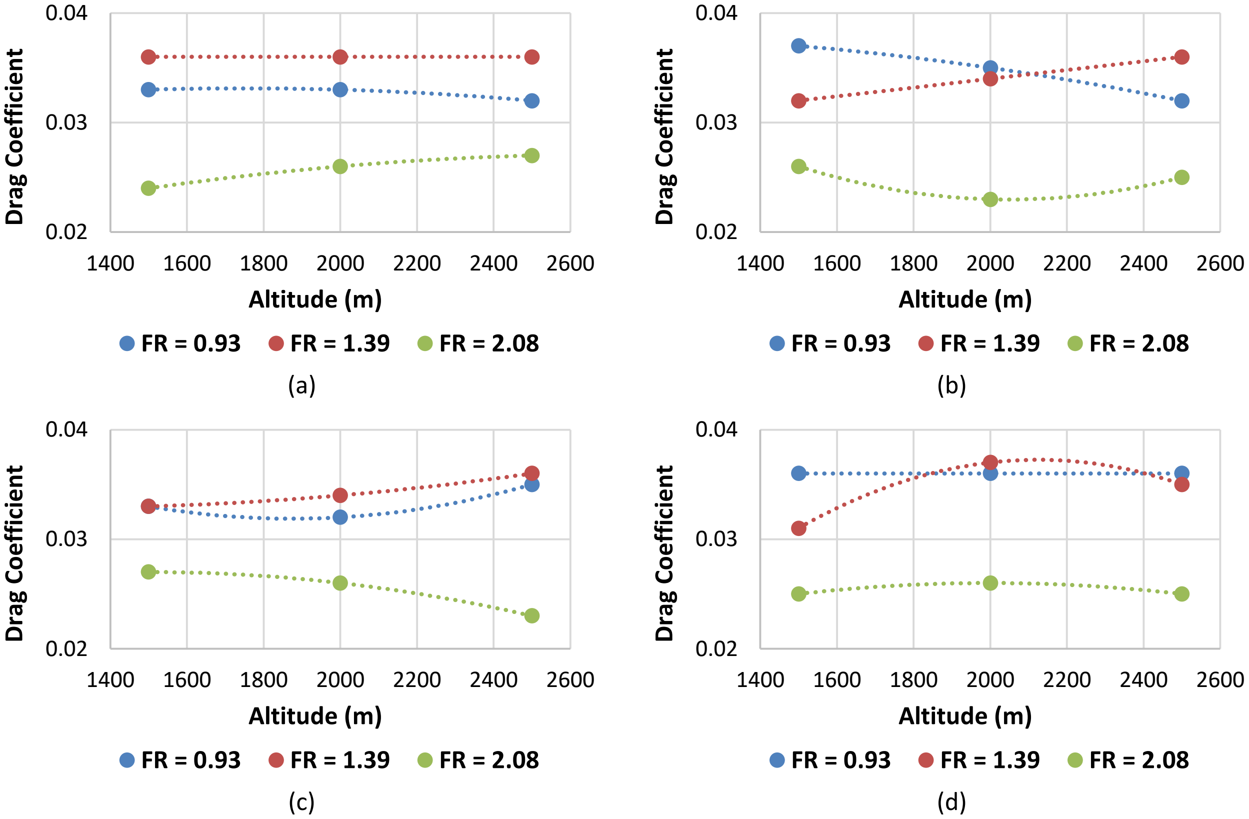

Fig. 13. Drag coefficient for different altitudes at (a) 100 km/h; (b) 140 km/h; (c) 190 km/h; (d) 250 km/h

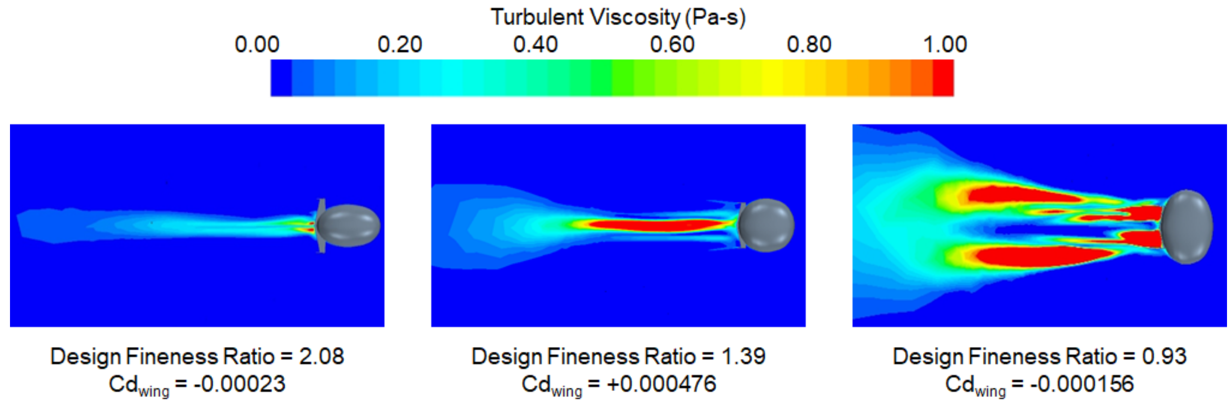

Fig. 14. Turbulent viscosity at altitude of 1500 m and velocity 140 km/h

It can be taken that the resultant drag is heavily influenced by the shape of the airship model and, in this case, by how the design scaling process is done to achieve the intended design fineness ratio. More positive drag force is generally produced as the altitude is decreased. In conclusion, it appears that altitude has a notable effect to the lift force generation but does not significantly affect the drag force magnitude for considered combination of design fineness ratio and velocity.

3.2 Effect of Velocity on Lift and Drag Coefficients

The effect of velocity to the generation of lift force is observed from the constructed plots based on CFD simulation results in Figure 15. In the plots, lift force generation was mostly increased with increasing velocity regardless of the altitude for design fineness ratios of 0.93 to 2.08. The percentage increment of lift coefficient for design fineness ratio of 0.93 at each altitude is the highest compared to other ratios.

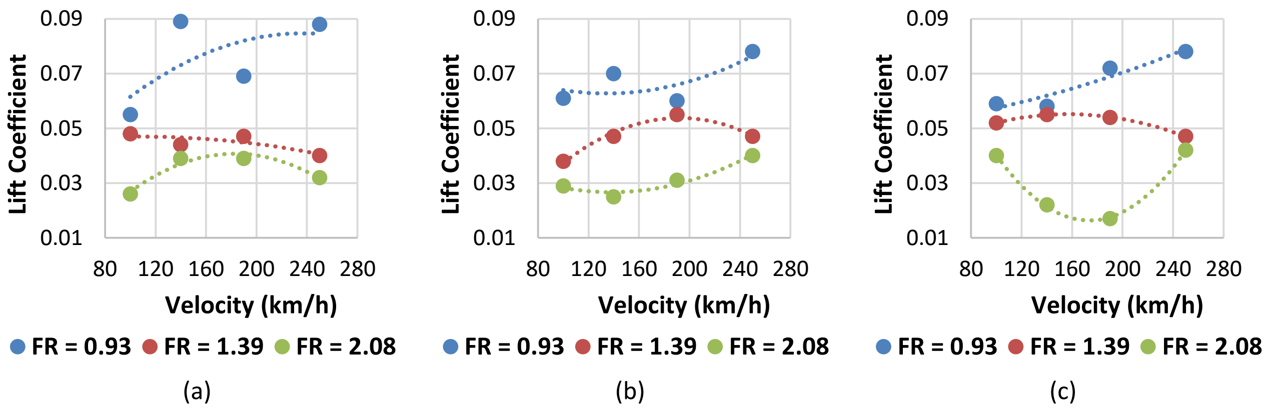

Fig. 15. Lift coefficient for different velocities at (a) 1500 m; (b) 2000 m; (c) 2500 m

Meanwhile, the effect of velocity to the generation of drag force is observed from the constructed plots based on the obtained CFD simulation results in Figure 16. From the plotted simulation results, the drag force can be taken to be essentially constant with increasing velocity at each altitude. This is in line with published results in the study by Sadraey [20], which indicates that the velocity has no considerable effect on the generated drag force when the Mach number is less than 0.7 because the compressible and wave drag effects around the body are small. The drag force can thus be considered constant in such cases. Since the velocity variation for this simulation study falls below that Mach number for each of the considered altitudes, this supports observed behaviour of the simulated drag.

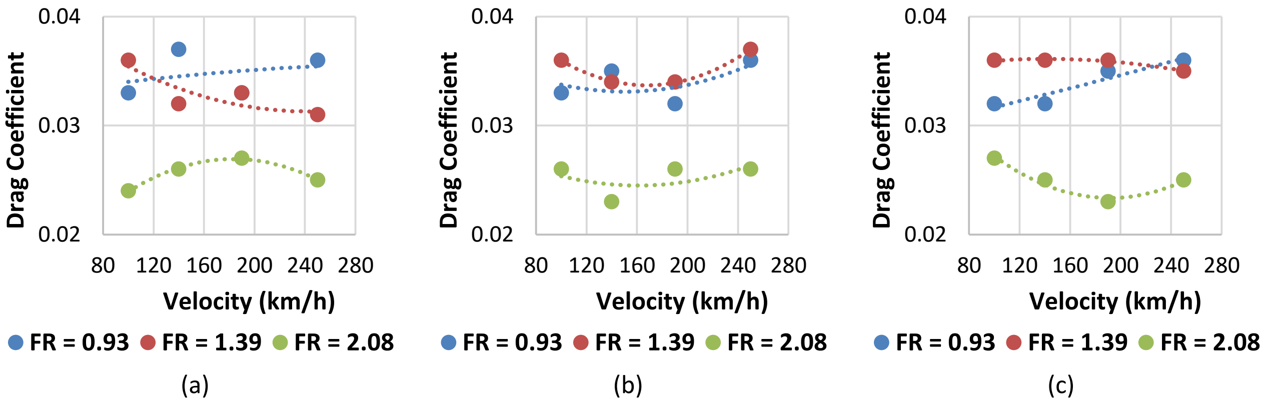

Fig. 16. Drag coefficient for different velocities at (a) 1500 m; (b) 2000 m; (c) 2500 m

It can be concluded that velocity has a rather notable effect on the lift force generation, especially at the lower altitudes. On the other hand, the drag force generation was rather consistent with the varying velocities, signifying a low impact of the velocity on drag force.

3.3 Effect of Fineness Ratio on Lift and Drag Coefficients

Figure 17 shows the variation of the lift coefficient as the velocity and altitude are changed. It can be observed that the airship model creates higher lift at design fineness ratio of 0.93 in comparison to the other ratios with variation of velocities and altitudes. In fact, the trend appears to indicate that the influence of design fineness ratio is more significant than velocity and altitude. The difference in lift force produced from different design fineness ratios is more pronounced as velocity increases and lower fineness ratio corresponds to higher lift force. A reason for this situation is because airship with low fineness ratio has a wider body that enables it to have more lifting surface to create more lift as highlighted in Figure 18. All in all, it can be taken that the airship with smaller fineness ratio is capable to generate more lift at all velocities and altitudes.

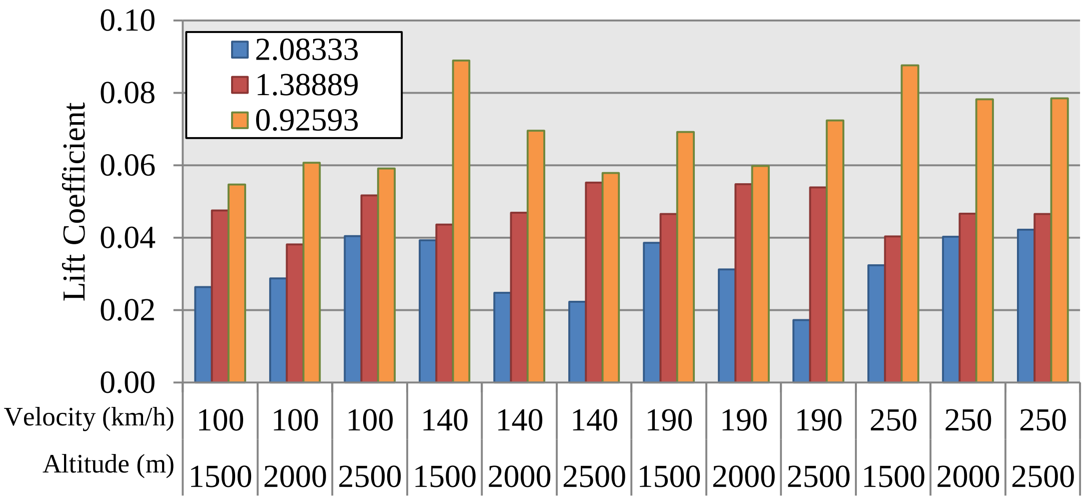

Fig. 17. Simulated value of lift coefficient for different design fineness ratios

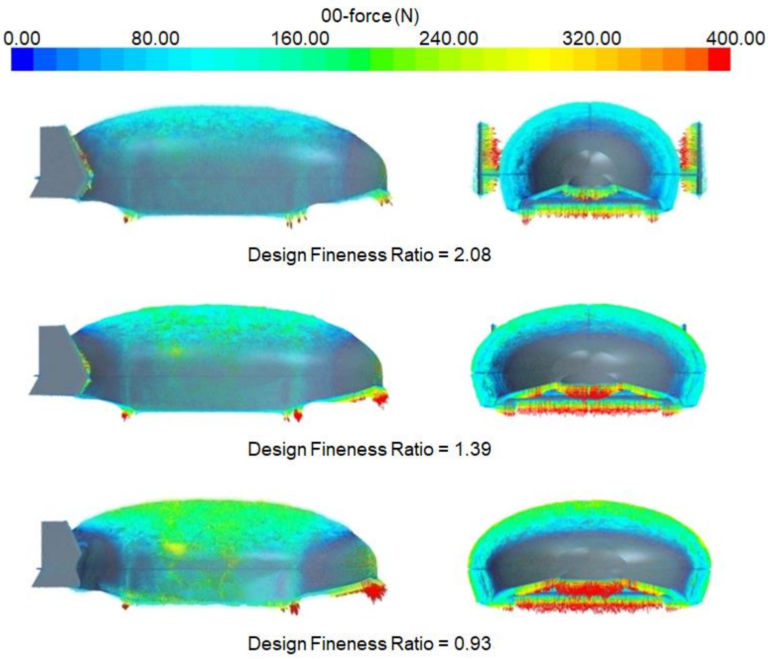

Fig. 18. Simulated normal force acting on airship body at 250 km/h and 2500 m altitude

In the meantime, Figure 19 shows the plot of simulated drag coefficient against design fineness ratio. It can be observed that the produced drag coefficient is within the range of 0.025 to 0.045. An interesting observation that can be noted is that the drag force generated with design fineness ratio of 1.39 is mostly higher than that obtained with design fineness ratio of 0.93 at several combinations of velocity and altitude. This situation occurs despite the fact that the airship will have smaller surface area at design fineness ratio of 1.39. A possible explanation for this can be contributed to the collision of airflow from the body surface to the wing, which creates large turbulence vortex as illustrated in Figure 20. Due to this condition, the wing is unable to reduce the pressure of airflow around it and this will increase the pressure drag. To improve this condition, the wing design must be configured appropriately with the changing design fineness ratio, which in this case study the wing configuration is maintained for all different fineness ratios. It can therefore be concluded that design fineness ratio definitely has a significant effect on both the lift and drag force generation of the airship design.

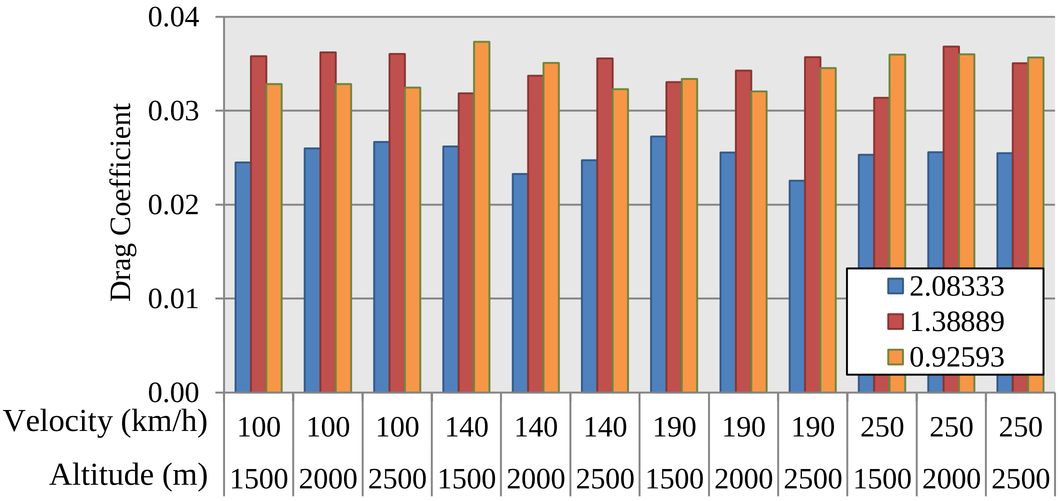

Fig. 19. Simulated value of drag coefficient for different design fineness ratios

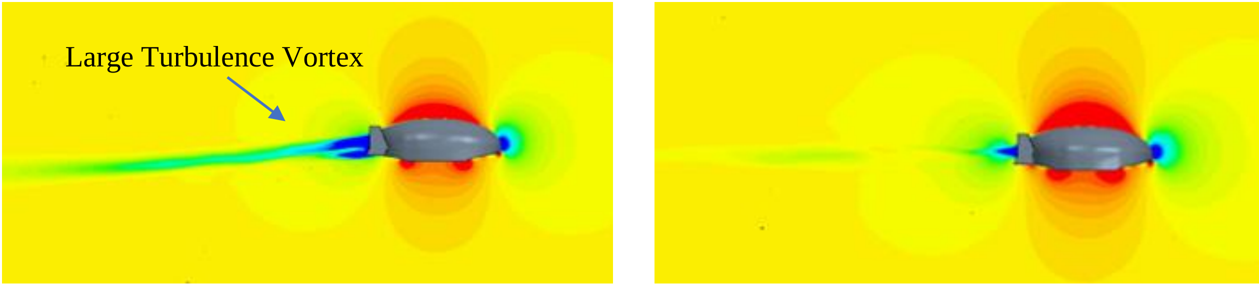

(a) (b)

Fig. 20. Simulation results at velocity 190 km/h and altitude 2000 m for (a) fineness ratio = 1.39; (b) fineness ratio = 0.93

3.4 Mathematical Modelling of Airship Performance

As previously observed, the trend of individual effects from the design fineness ratio, altitude and velocity are not readily visible. Subsequently, the combinatorial effects from these three parameters will be much harder to predict manually. To ease this situation, mathematical modelling of the effects can be developed using the simulated CFD data for lift and drag forces with different combinations of design fineness ratio, velocity and altitude. The MINITAB statistical software is utilized here for the equation fittings.

The simulated lift coefficient data was analysed and the resultant linear regression model of the lift coefficient against all predictor variables (i.e. design fineness ratio, velocity and altitude) is shown by Eq. (1), in which CL = lift coefficient, FR = airship's design fineness ratio, A = altitude (m) and V = velocity (km/h). It should be noted that the backward elimination method with alpha = 0.1 is used in fitting this regression model.

$$\begin{aligned} CL = & -7.2*10^{-1}*FR+9.7*10^{-3}*V+2.9*10^{-1}*FR^2-6.7*10^{-5}*V^2+2.4*10^{-4}*FR*A \\ & +2.6*10^{-3}*FR*V-3.8*10^{-6}*A*V+1.6*10^{-7}*V^3-1.0*10^{-4}*FR^2*A-1.9*10^{3}*FR^2*V \\ & +3.3*10^{-10}*A^2*V+1.9*10^{-8}*A*V^2+1.5*10^{-8}*FR^2*A^2+6.0*10^{-6}*FR^2*V^2 \\ & -3.3*10^{-10}*FR*A^2*V+3.7*10^{-9}*FR*A*V^2-4.7*10^{-8}*FR*V^3-4.2*10^{-11}*A*V^3 \end{aligned} \quad (1)$$

The p-value in analysis of variance (ANOVA) for the regression model fitting of the lift coefficient is very small, which is very close to 0, and this indicates that the model explains the variation in the value of the generated lift coefficient very well. However, before this resultant regression model in Eq. (1) can be used for prediction of lift coefficient value with varying airship's design fineness ratio, velocity and also altitude, the mathematical model has to be checked for its goodness of fit. The first goodness-of-fit test is R^2 value or coefficient of determination. For this case of Eq. (1), the R^2 value is 99.3%. In other words, this can be interpreted that roughly 99.3% of the lift coefficient data variability within the considered range of the predictor variables is appropriately captured by the regression model. This is also reflected by the plot of observed versus fitted responses for the lift coefficient shown in Figure 21, where it is observed that the data points are aligned in almost straight line. This indicates good agreement between the observed and fitted values of lift coefficient, hence a good fit of the regression model. Moreover, goodness of fit for the constructed regression model can also be tested by looking at the residual plots in Figure 22. The residuals do not indicate any visible trend and the data points are randomly scattered, which implies there is no significant higher order term that must be included in the model. Moreover, the histogram of residuals closely resembles that of the normal distribution, which matches the assumption made in standard linear regression method.

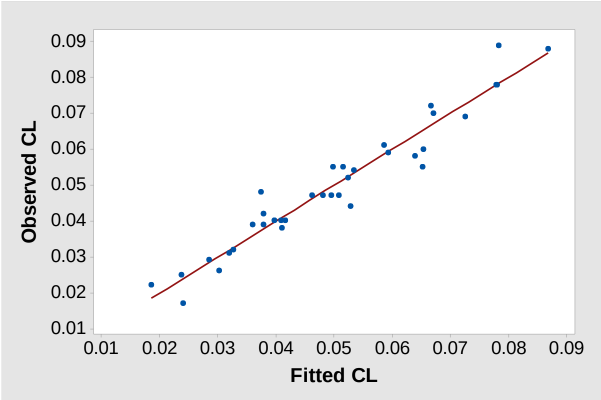

Fig. 21. Plot of observed versus fitted lift coefficient values

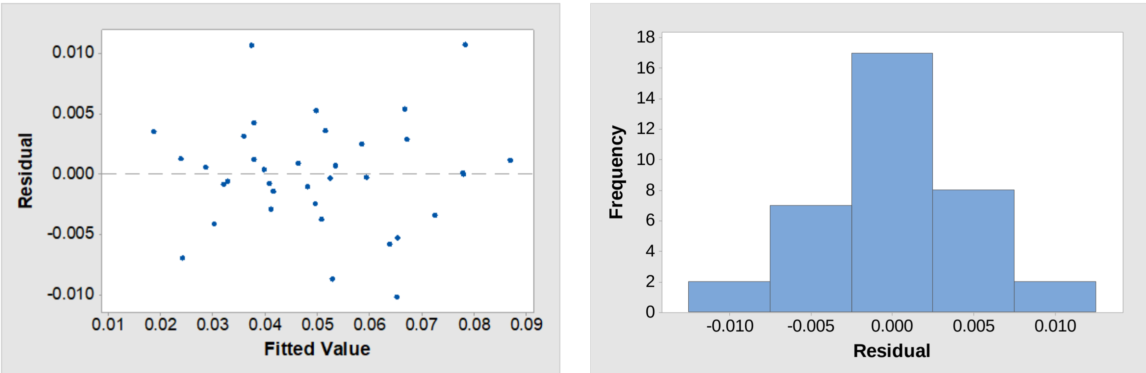

Fig. 22. Plot of residuals for lift coefficient model

Last but not least, the verification of the regression model for the lift coefficient is done using few random sample cases. The selected random simulation results from the CFD analysis in StarCCM+ are tabulated in Table 6 with comparison to the fitted lift coefficient values using the regression model. It can be observed that the error percentage is very small between the two values, with the maximum is only about 5%. This can be taken as a good indication that the constructed regression model has effectively captured the relationship between the generated lift coefficient and all of the considered predictors: design fineness ratio, velocity and altitude.

Table 6
Comparison of random test cases for lift coefficient model

Fineness Ratio	Altitude (m)	Velocity (km/h)	Simulated CL	Fitted CL	% Error
1.19	1800	120	0.0548	0.0549	0.2126
1.19	2400	240	0.0597	0.0595	0.3785
1.04	1800	120	0.0652	0.0622	4.5554
1.04	2200	180	0.0586	0.0617	5.2464
1.04	2400	240	0.0694	0.0673	3.0577

In similar fashion, the simulated drag coefficient data from StarCCM+ software is analyzed and the resultant linear regression model of the drag coefficient against all predictor variables (i.e. design fineness ratio, velocity and altitude) is indicated by Eq. (2), where CD = drag coefficient, A = altitude (m), FR = airship's design fineness ratio and V = velocity (km/h). It should be noted that the backward elimination method with alpha = 0.1 is used in fitting this regression model.

$$CD = 4.5*10^{-4}*V - 5.0*10^{-9}*A^2 + 2.1*10^{-6}*V^2 + 3.0*10^{-5}*FR*A - 1.7*10^{-4}*FR*V$$
$$+ 4.1*10^{-9}*V^3 - 1.2*10^{-5}*FR^2*A + 5.2*10^{-5}*FR^2*V + 5.3*10^{-10}*FR^2*A^2 \quad (2)$$

The p-value in analysis of variance (ANOVA) for the regression model fitting of drag coefficient is very small, which is close to 0, and this indicates that the model explains the variation in value of the generated drag coefficient very well. Goodness of fit for the drag coefficient model is also established from several tests. Its R^2 value is found to be 99.8%, which implies that 99.8% of the drag coefficient data variability is appropriately captured by the regression model. This is also reflected by the plot of observed versus fitted responses for the drag coefficient in Figure 23, where it can be observed that the data points are aligned in an almost straight line. This indicates a good agreement between the observed and fitted values of drag coefficient, hence a good fit of the regression model.

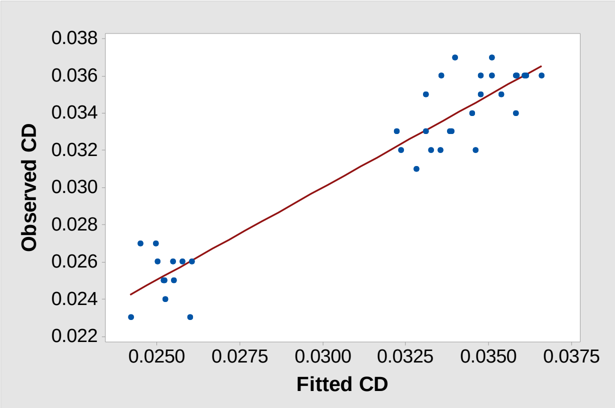

Fig. 23. Plot of observed versus fitted drag coefficient values

Moreover, the goodness of fit for the regression model can also be indicated from its illustrated residual plots in Figure 24. The residual plots do not indicate any visible trend and the data points are randomly scattered. This is a good situation, which implies that there is no significant higher order term that must be included into the model. Plus, the histogram of the residuals also closely resembles normal distribution, which matches the assumption made in linear regression method.

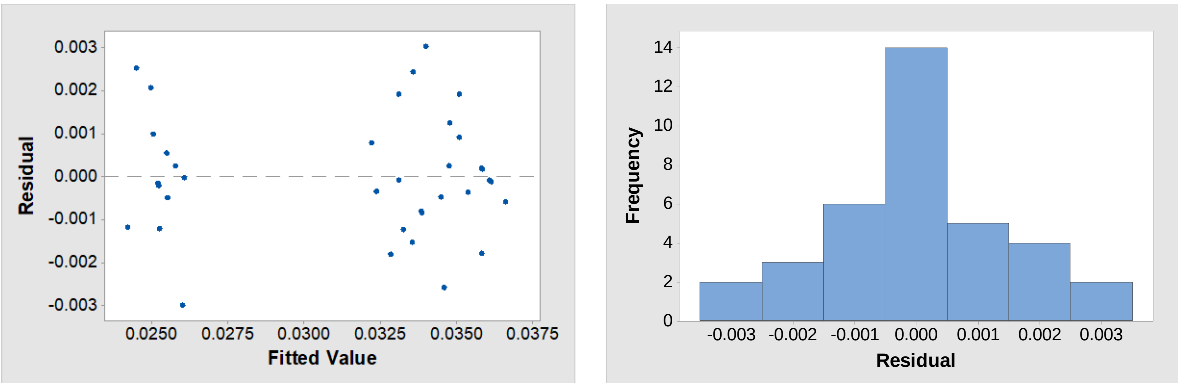

Fig. 24. Plot of residuals for drag coefficient model

The verification of the regression model for drag coefficient is done using several random sample cases. The outputs from the random CFD simulation of the points selected are tabulated in Table 7, along with the comparison with the fitted drag coefficient values using the regression model. It can be observed that the error percentage is very small between the two values, which the maximum is only about 11%, and this can be taken as a sign that the regression model appropriately captures the relationship between the generated drag coefficient and all considered predictors.

Table 7
Comparison of random test cases for drag coefficient model

Fineness Ratio	Altitude (m)	Velocity (km/h)	Simulated CD	Fitted CD	% Error
1.19	1800	120	0.0353	0.0357	1.1073
1.19	2400	240	0.0401	0.0356	11.1966
1.04	1800	120	0.0381	0.0352	7.5523
1.04	2200	180	0.0356	0.0350	1.6594
1.04	2400	240	0.0366	0.0354	3.3016

3.5 Summary of Findings

At this point, the CFD simulation work on aerodynamic performance (i.e. lift and drag coefficient) of the selected reference airship model with varying design fineness ratio, velocity and altitude were presented and discussed. Using the simulation results, the mathematical regression models that can appropriately relate the generation of lift and drag forces with different settings of design fineness ratio, velocity and altitude were derived and their goodness in predicting aerodynamic performance of the airship was also verified. At this point, it can be concluded that design fineness ratio does have significant impact on aerodynamic performance of the airship, which was reflected by the simulation results and statistical analysis of the regression model. In general, it was found that for the chosen approximate Atlant-100 airship model, both aerodynamic lift and drag forces will increase as design fineness ratio is made smaller. All in all, based on the observation of the simulated results, fineness ratio of 0.93 corresponds to the highest lift coefficient while the effect of wing drag causes fineness ratio of 1.39 to mostly have the highest drag when both velocity and altitude increases. Hence it can be taken that a low design fineness ratio may be more preferable for this airship model.

4. Conclusion and Future Works

CFD simulation analysis using StarCCM+ software has been conducted to obtain the aerodynamic performance characteristics of approximate model of the Atlant-100 airship design. The simulation results obtained appear to indicate that the generated lift and drag forces are affected by the varying design fineness ratio, velocity and altitude. This finding is further strengthened through the statistical analysis of the obtained simulation data where mathematical models for the lift and drag forces are derived. In general, for the chosen approximate Atlant-100 airship model, both of the generated lift and drag forces will increase as design fineness ratio is made smaller. However, it should be carefully noted that this result is extremely influenced by the design shape of the airship model. Although it is believed that the general trend of the effects from varying fineness ratio on the airship's aerodynamic performance is mostly similar for the other conventional airship designs, the derived mathematical models are only applicable and specific to the chosen approximate Atlant-100 airship model used in this study. Based on the results, fineness ratio of 0.93 corresponds to a higher lift coefficient whereas the effect of wing drag causes fineness ratio of 1.39 to have a higher drag when velocity and altitude increases. It is concluded from the simulation results and established regression models that design fineness ratio has significant impact on the generated lift and drag forces on the airship, which is also evidently higher than that of altitude and velocity. Fineness ratio generates the largest contributing factor in linear regression models for lift and drag coefficients that have passed goodness of fit tests.

For future works, it should be noted that the change in external shape of the airship design will be different if the changes in fineness ratio is achieved through other ways of design modification of the airship model than the one applied in this study. It would be interesting to study whether the effects of design fineness ratio found in this study remains similar when different design changes are made. Furthermore, the complete airship design can be described by several other parameters such as the wing and engine design parameters. In order to capture the whole essences on how design of the airship will influence its aerodynamic performance, all these parameters need to be considered as well. Last but not least, hybrid turbulent model can be used in future study because it can better capture the aerodynamic forces in the analysis research. This comes at the expense of more required research time and powerful computing tool for the analysis. Nevertheless, to obtain more accurate representation of aerodynamic performance, this can be considered as an extension of this study.

Acknowledgement
This research was not funded by any grant.

References

[1] Prentice, Barry E., Richard E. Beilock, Alfred J. Phillips, and Jim Thomson. "The rebirth of airships." In *Journal of the Transportation Research Forum*, vol. 44, no. 1. 2010. https://doi.org/10.5399/osu/jtrf.44.1.806

[2] Aminian, Negin O., and Fairuz I. Romli. "Study on the Potential of Airships as Urban Mass Public Transport in Malaysia." *Journal of Mechanical Engineering* (2017): 221-232.

[3] Unal, Resit, Roger Lepsch, and Mark McMillin. "Response surface model building and multidisciplinary optimization using D-optimal designs." In *7th AIAA/USAF/NASA/ISSMO Symposium on Multidisciplinary Analysis and Optimization*, p. 4759. 1998. https://doi.org/10.2514/6.1998-4759

[4] Sahai, Amal, Bibin John, and Ganesh Natarajan. "Effect of fineness ratio on minimum-drag shapes in hypersonic flows." *Journal of Spacecraft and Rockets* 51, no. 3 (2014): 900-907. https://doi.org/10.2514/1.A32583

[5] Kruger, Michael, R. J. Huyssen, L. Smith, and J. P. Meyer. "Application of a low fineness ratio fuselage to an airliner configuration." In *54th AIAA Aerospace Sciences Meeting*, p. 1282. 2016. https://doi.org/10.2514/6.2016-1282

[6] Nicolosi, Fabrizio, Pierluigi Della Vecchia, Danilo Ciliberti, and Vincenzo Cusati. "Fuselage aerodynamic prediction methods." *Aerospace Science and Technology* 55 (2016): 332-343. https://doi.org/10.1016/j.ast.2016.06.012

[7] Munk, Max M. "Aerodynamics of airships." In *Aerodynamic theory*, pp. 32-48. Springer, Berlin, Heidelberg, 1936. https://doi.org/10.1007/978-3-642-91484-3_2

[8] Andan, Amelda D., Waqar Asrar, and Ashraf A. Omar. "Investigation of aerodynamic parameters of a hybrid airship." *Journal of Aircraft* 49, no. 2 (2012): 658-662. https://doi.org/10.2514/1.C031491

[9] Wang, Xiao-Liang, Gong-Yi Fu, Deng-Ping Duan, and Xue-Xiong Shan. "Experimental investigations on aerodynamic characteristics of the ZHIYUAN-1 airship." *Journal of aircraft* 47, no. 4 (2010): 1463-1468. https://doi.org/10.2514/1.C000243

[10] Sun, Xiao-Ying, Tian-E. Li, Guo-Chang Lin, and Yue Wu. "A study on the aerodynamic characteristics of a stratospheric airship in its entire flight envelope." *Proceedings of the Institution of Mechanical Engineers, Part G: Journal of Aerospace Engineering* 232, no. 5 (2018): 902-921. https://doi.org/10.1177/0954410017723358

[11] Jalasabri, J., and F. Romli. "Computational Fluid Dynamics (CFD) Study on a Hybrid Airship Design." *International Review of Mechanical Engineering* 11, no. 8 (2017). https://doi.org/10.15866/ireme.v11i8.11645

[12] Ashham, M., A. M. Aliywy, S. H. Raheemah, K. Salman, and M. Abbas. "Computational Fluid Dynamic Study on Oil-Water Two Phase Flow in A Vertical Pipe for Australian Crude Oil." *Journal of Advanced Research in Fluid Mechanics and Thermal Sciences* 71, no. 2 (2020): 134-142. https://doi.org/10.37934/arfmts.71.2.134142

[13] Kunya, Bashir Isyaku, Clement Olaloye Folayan, Gyang Yakubu Pam, Fatai Olukayode Anafi, and Nura Mu'az Muhammad. "Performance study of Whale-Inspired Wind Turbine Blade at Low Wind Speed Using Numerical Method." *CFD Letters* 11, no. 7 (2019): 11-25.

[14] Rahman, M. A., M. Y. Harmin, M. F. S. Koslan, M. R. Saad, F. I. Romli, and M. T. Ahmad. "Size-scale effects of inboard Store-Y on X-plane model: A parametric study using CFD." *MS&E* 270, no. 1 (2017): 012006. https://doi.org/10.1088/1757-899X/270/1/012006

[15] Jespersen, Dennis C., Thomas H. Pulliam, and Marissa Lynn Childs. "Overflow turbulence modeling resource validation results." (2016).

[16] Ahmed, Tousif, Md Tanjin Amin, SM Rafiul Islam, and Shabbir Ahmed. "Computational study of flow around a NACA 0012 wing flapped at different flap angles with varying Mach numbers." *Global Journal of Research in Engineering* 13, no. 4 (2013): 5–14

[17] Eleni, Douvi C., Tsavalos I. Athanasios, and Margaris P. Dionissios. "Evaluation of the turbulence models for the simulation of the flow over a National Advisory Committee for Aeronautics (NACA) 0012 airfoil." *Journal of Mechanical Engineering Research* 4, no. 3 (2012): 100-111. https://doi.org/10.5897/JMER11.074

[18] Voloshin, Vitaly, Yong K. Chen, and Rajnish K. Calay. "A comparison of turbulence models in airship steady-state CFD simulations." *arXiv preprint arXiv:1210.2970* (2012).

[19] Battipede, Manuela, P. Gili, and M. Vazzola. "Structural and aerodynamics analysis on different architectures for the elettra twin flyer prototype." *Journal of Intelligent & Robotic Systems* 72, no. 1 (2013): 123-144. https://doi.org/10.1007/s10846-013-9823-9

[20] Sadraey, Mohammad. *Aircraft performance: analysis*. VDM Publishing, 2009.